Supporting Information

High-Efficiency Air-Stable Colloidal Quantum Dot Solar Cells Based on Potassium Doped ZnO Electron Accepting Layer

Randi Azmi,[†] *Gabseok Seo,*[‡] *Tae Kyu Ahn,*[‡] *and Sung-Yeon Jang*[†*]

[†]Department of Chemistry, Kookmin University, 77 Jeongneung-ro, Seongbuk-gu, Seoul 136-702, Republic of Korea

[‡] Department of Energy Science, Sungkyunkwan University, 2066 Seobu-ro, Jangan-gu, Suwon, Gyeonggi-do 16419, Republic of Korea

Email: syjang@kookmin.ac.kr

Experimental section

Synthesis of PbS-CQD: Lead oxide (PbO trace-metals basis, 99.999%), hexamethyldisilathiane (TMS2S, synthesis grade), oleic acid (OA, technical grade, 90%), 1-octadecene (ODE, 90%), olaylamine and 1,3-propanedithiol (PDT, >99%) were purchased from Sigma-Aldrich and used without further purification. The oleate-capped PbS-CQD was synthesized via a rapid hot injection method by following a reported procedure with slight modification.[S1] Briefly, 2 mmol of PbO and 4 mmol of OA were dissolved in 20 mL of ODE in a three-necked flask by heating the mixture to 100 °C and keeping it under vacuum overnight. A portion (180 μL) of TMS2S in ODE was injected into the lead oleate solution under N_2 gas. The PbS-CQDs were then purified by adding 40 mL acetone one time and then the precipitate was diluted in toluene (150 mg/mL) for the next solution-phase halide treatment. The solution-phase treatment using PDMII ligand was adapted from a previous article.[S2] Finally, the precipitate was dried in a vacuum chamber to remove any residual solvent before dilution in octane (70 mg/mL).

Photovoltaic device fabrication: The ITO/glass substrates were cleaned sequentially in acetone and isopropyl alcohol for 15 min each. After drying in a vacuum oven, the ITO/glass substrates were put in the UV ozone chamber for 20 min prior to use. The ZnO-ETLs were prepared by the in situ sol-gel method described in our previous articles.[S3-S5] The ZnO was spin-cast at 2000 rpm and then annealed at 130 ℃ to get thickness of ≈40 nm. A 15 mM solution of KOH in deionized (DI) water was prepared, and then the ZnO-ETL film was dipped for 1 min followed by washing with DI water and annealing at 100 ℃. PbS-CQD active layers were deposited using a conventional layer-by-layer (LBL) spin coating process under ambient atmosphere. A PbS-CQD solution (30 μl in octane) was dropped and spin-coated at 2000 rpm for 10 sec following solid-state exchange (SSE) using 4 mM PDMII solution in ethanol until reaching a thickness of ≈250 nm (four layer-cycles). Two wash cycles were done for each layer to remove unbound ligands at 2000 rpm with the same program. A conventional thin layer of PDT-exchanged PbS-CQD (thickness ≈50 nm, 1 layer-cycle) was used as a hole-accepting layer. The

concentration of PDT was 2 mM in acetonitrile. The unbound ligands were removed by two wash cycles with acetonitrile. The 100 nm-thick Au used as anode was deposited using thermal evaporation at low pressure (<10^{-6} Torr).

Device Analysis: The current density-voltage (*J-V*) characteristics were determined using a Keithley 2401 source unit under the light intensity AM 1.5 G (100 mWcm^{-2}) illumination (Newport). The spectral mismatch was calibrated using a KG-5 filter-covered mono-silicon standard cell (Newport). A metal mask was used with active area 0.0518 cm^2. External quantum efficiency (EQE) spectra were obtained by passing the output of a 400 W Xenon lamp through a monochromator and filters. The collimated output of the monochromator was measured through a 1 mm aperture (ORIEL, QuantX 300). The calibration was performed using a 603621 Calibrated Silicon and Germanium Reference Detector. The wavelength values were scanned at chopping frequency of 4 Hz from 300 nm to 850 nm. Transient photo-voltage (TPV) measurements (McScience, K3400) were performed at steady state under continuous illumination. The system was perturbed using a green (λ = 535 nm) pulsed laser at 1 Hz. The resulting voltage transient was acquired using a DPO 3052 Tektronix Digital Phosphor Oscilloscope (impedance 1 MΩ). The recombination lifetime was extracted from the decay curves using mono-exponential fitting. Capacitance–voltage (*C*p–*V*) measurement of solar cell devices was performed using an impedance analyzer (Ivium Stat.) in dark and the AC signal was set to 1 kHz frequency. The depletion width was calculated using the equation (S1):

$$W_{\mathrm{D}}(\mathrm{V}) = \frac{1}{N_{\mathrm{a}}}\sqrt{\frac{2\epsilon_r\epsilon_0(V_{bi}-V)}{e(\frac{1}{N_{\mathrm{a}}}+\frac{1}{N_b})}} \qquad \text{(S1)}$$

where ϵ_r is the PbS-CQDs dielectric constant (ϵ_r = 18), N_{a} is the PbS-CQDs doping density, N_{b} is the ZnO doping density, e is the elementary charge of an electron and V_{bi} is the built-in potential of our devices. The ZnO doping density is 10^{17} cm^{-3}. The built-in potentials (V_{bi}) and

doping density (N_a) of the PbS-CQDs active layers were obtained from a Mott-Schottky plot following equation S2.

$$\frac{1}{C^2} = \frac{2\,(V_{bi}-V)}{A^2 e \epsilon_r \epsilon_0 N_a} \qquad \text{(S2)}$$

Long-term Air Storage Stability Test: Unencapsulated devices were stored in darkness and ambient air. The devices were measured under AM 1.5G one-sun illumination (100 $mWcm^{-2}$) for every few days until 90 days. The relative humidity was in the range 43 ± 3 %, and temperature was 25 ± 2 ℃. After each measurement, the devices were returned to darkness.

Photo-stability test: A continuous photo-stability test was performed under AM 1.5G one-sun illumination without any filter. The relative humidity was in the range 40 ± 2 % and temperature 48 ± 2 ℃. All devices were unencapsulated and the measurements were performed every several minutes at the maximum power point.

Sample Analysis: XPS was performed using a MultiLab 2000 (THERMO VG SCIENCE) system equipped with monochromatized Mg Kα radiation at hv = 1253.6 eV. The base pressure was 1×10^{-9} Pa. UPS measurements were performed using an AXIS-NOVA (Kratos) system with HeIα radiation (hv = 21.22 eV) and a base pressure of 5×10^{-8} Torr. WF was calculated following the equation WF = 21.22 – cutoff region from the high binding energy (eV). The FE-SEM images were taken using a JSM-7610F (JEOL) field-emission scanning electron microscope (FESEM). Photoluminescence measurements were carried out using an SPEX Nanolog 3-211 (Horriba). The signal was analyzed using an NIR spectrometer equipped with an InGaAs array detector (Symhony II). The mobility of ZnO-EAL was characterized using the space charge limited current (SCLC) analysis. The structure of electron-only device was glass/ITO/ZnO/Al. To secure the space charge limited region, 300 nm thickness of ZnO-EALs was used. The Mott-Gurney equation was used to obtain the mobility at trap-free regime following:

$$J = \frac{9\mu\epsilon_0\epsilon_r V^2}{8L^3} \qquad \text{(S3)}$$

where *J* is the current density, μ is the mobility, ϵ_0 is the permittivity under vacuum, ϵ_r is the dielectric constant of ZnO, L is the film thickness and V is the applied bias.

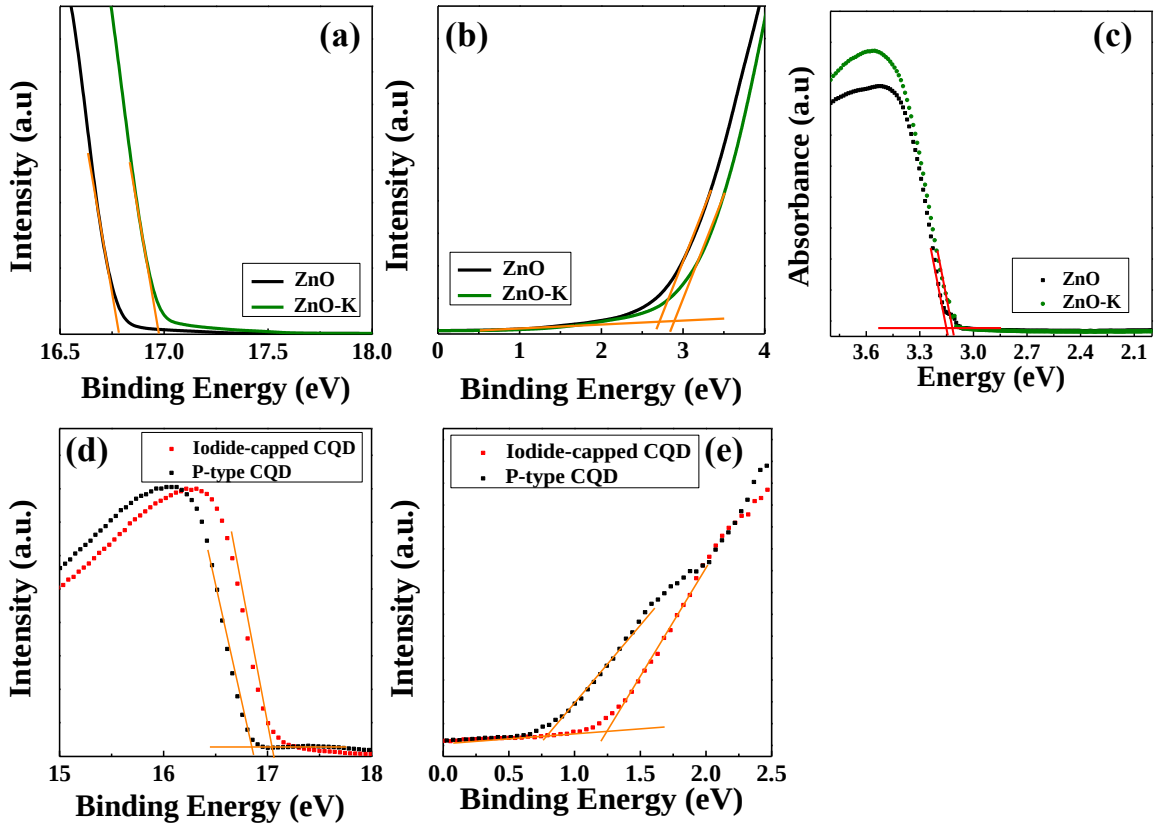

Figure S1. UPS analysis results of pristine ZnO and ZnO-K films: (a) Secondary electron cut-off region and (b) Low binding energy region; (c) Absorption spectra of pristine ZnO and ZnO-K films. UPS analysis results of PbS-CQDs: (d) Secondary electron cut-off region; and (e) Low binding energy region.

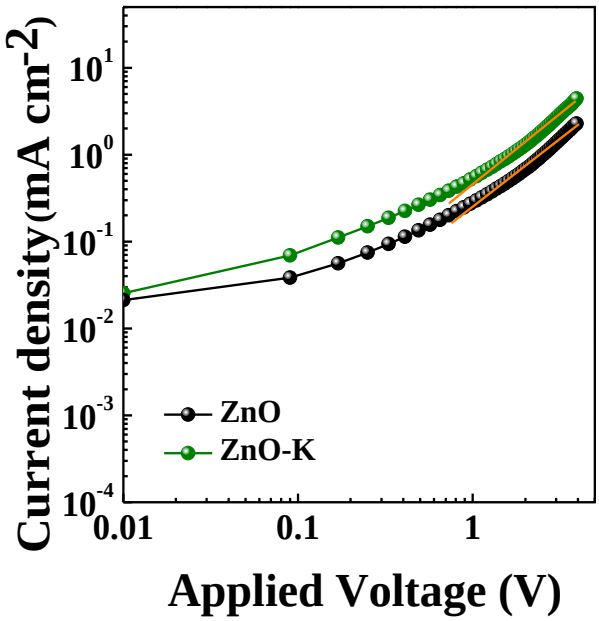

Figure S2. Mott-Gurney plot of various ZnO-EALs by SCLC analysis.

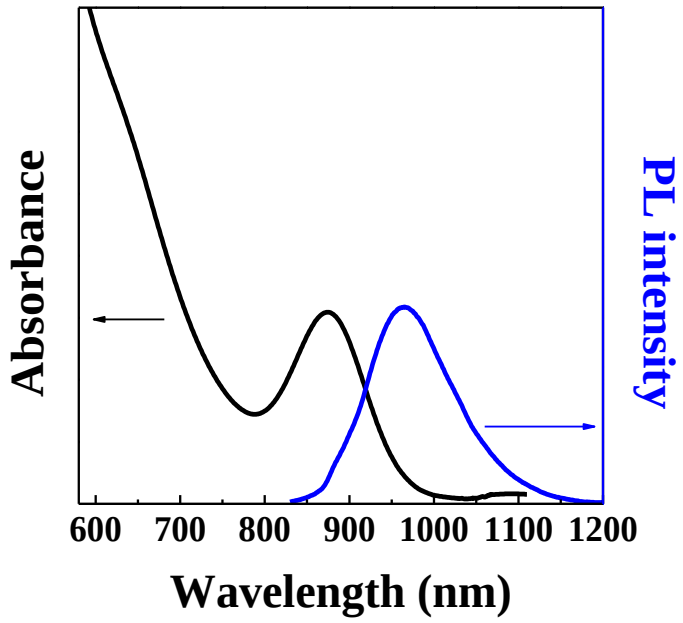

Figure S3. UV-vis absorption and PL emission spectrum of the oleate-capped PbS-CQD used in this study.

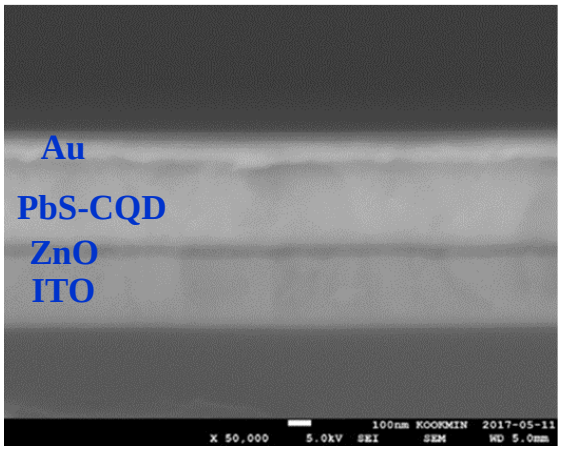

Figure S4. Cross-sectional SEM image of a CQDSC device.

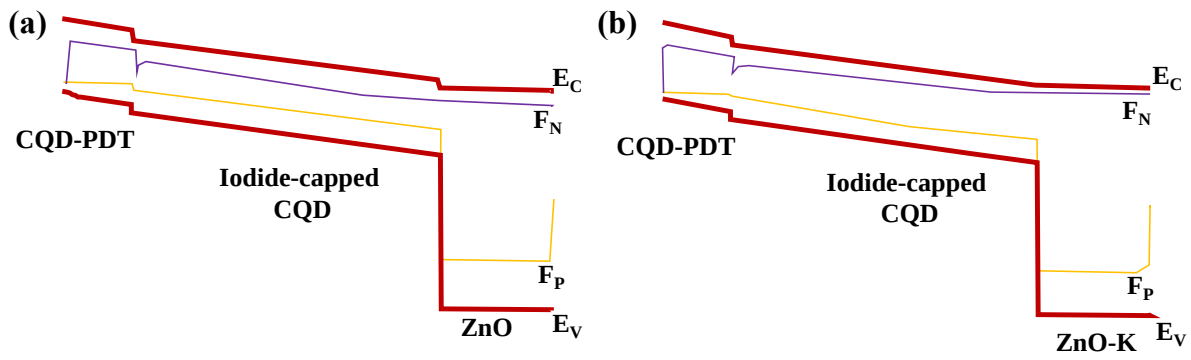

Figure S5. Energy band-bending diagram of CQDSCs using (a) pristine ZnO and (b) ZnO-K as the EAL, at short-circuit condition.

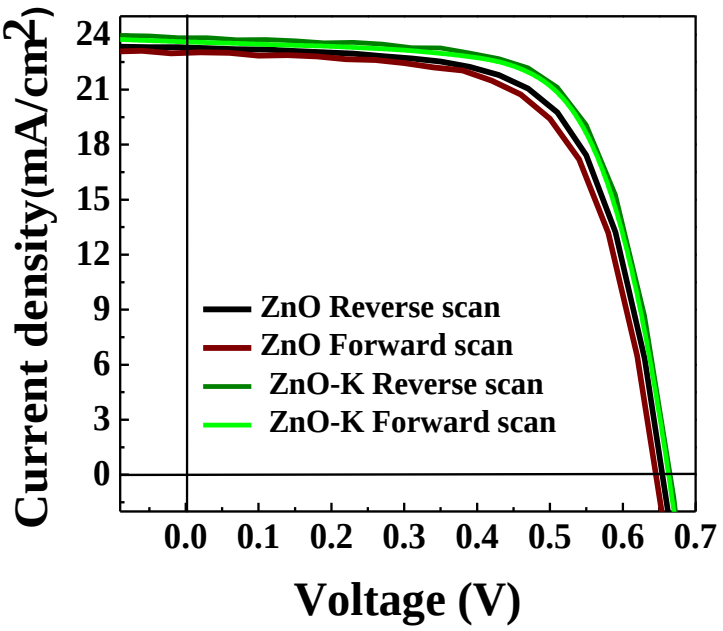

Figure S6. *J-V* characteristics of devices using pristine ZnO and ZnO-K under reverse and forward scans.

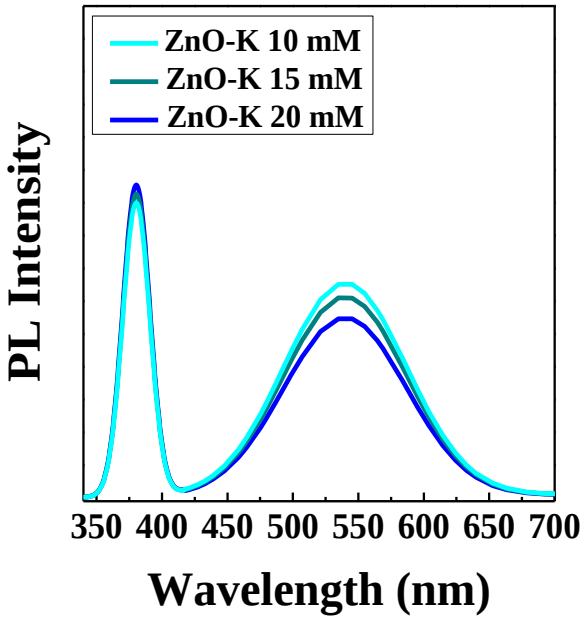

Figure S7. PL spectra of ZnO-K treated with various KOH solutions.

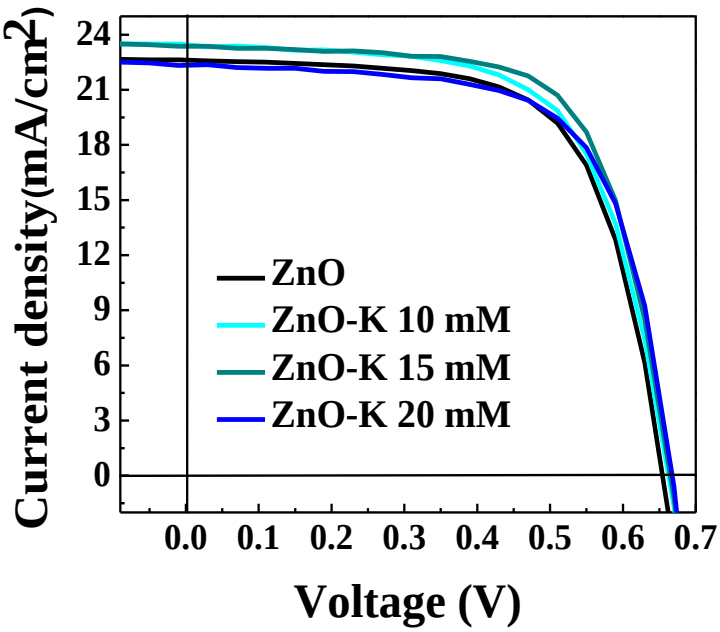

Figure S8. *J-V* characteristics of ZnO-K based CQDSCs with various KOH solutions.

Table S1. Summary of performance CQDSCs with various KOH solutions.

EAL	PCE (%)	V_{OC} (V)	J_{SC} (mA cm^{-2})	FF
ZnO	9.62	0.64	22.78	0.65
ZnO-K 10 mM	10.12	0.65	23.41	0.66
ZnO-K 15 mM	10.47	0.66	23.38	0.67
ZnO-K 20 mM	9.28	0.66	22.53	0.63

SI REFERENCES

(S1) Hines, M.A.; Scholes, G.D. Colloidal PbS Nanocrystals with Size-Tunable Near-Infrared Emission: Observation of Post-Synthesis Self-Narrowing of the Particle Size Distribution. *Adv. Mater*. **2003**, *15*, 1844–1849.

(S2) Azmi, R.; Septy, S.; Aqoma, H.; Seo, G.; Ahn, T. K.; Park, M.; Ju, S.-Y.; Lee, J.-W.; Kim, T.-W.; Oh, S.-H.; Jang, S.-Y. Highly Efficient Air-Stable Colloidal Quantum Dot Solar Cells by Improved Surface Trap Passivation. *Nano Energy* **2017**, *39*, 86–94.

(S3) Azmi, R.; Hadmojo, W. T.; Sinaga, S.; Lee, C.-H.; Yoon, S. C.; Jung, I. H.; Jang, S.-Y. High-Efficiency Low-Temperature ZnO Based Perovskite Solar Cells Based on Highly Polar, Nonwetting Self-Assembled Molecular Layers. *Adv. Energy Mater*. **2018**, *8*, 1701683.

(S4) Azmi, R.; Nam, S.Y.; Sinaga, S.; Oh, S.-H.; Ahn, T. K.; Yoon, S. C.; Jung, I. H.; Jang, S.-Y. Improved Performance of Colloidal Quantum Dot Solar Cells Using High Electric-Dipole Self-Assembled Layers. *Nano Energy* **2017**, *39*, 355–362.

(S5) Azmi, R.; Nam, S.Y.; Sinaga, S.; Akbar, Z. A.; Lee, C.-H.; Yoon, S. C.; Jung, I. H.; Jang, S.-Y. High-Performance Dopant-Free Conjugated Small Molecule-Based Hole-Transport Materials for Perovskite Solar Cells. *Nano Energy* **2018**, *44*, 191–198.